X-Ray Crystallography: Bragg, Laue & Debye-Scherrer Methods

Natan Szczepaniak

March 2019

Abstract

Using a PHYWE X-Ray Unit Bragg's Method of X-Ray Diffraction is used to find the lattice constants and the densities of: Sodium Chloride ρ_{NaCl}=2.0957±0.0001 kgm^{-3}, Lithium Fluoride ρ_{LiF}=2.9656±0.0002 kgm^{-3} and Potassium Bromide ρ_{KBr}=2.2767±0.0006 kgm^{-3} which on average is 11% from the confirmed values. Various methods of improving the experiment are explored. Laue imaging is demonstrated in the purpose of finding the symmetry and structure of these crystals. Debye-Scherrer method of powder diffraction is also used to obtain diffraction pattern images of disordered crystals.

1 Introduction

X-Ray Crystallography (XRC) is one of the most fundamental techniques used in various scientific fields to study the structure and properties of periodic structures at the atomic level. Since the discovery of diffraction of X-Rays in crystalline structures by Lawrence and William Bragg in 1915, the technique has been used to determine the respective positions of atoms inside a crystal, electron densities and chemical bonds [1]. Together with XRC methods developed by Max von Laue, Peter Debye and Paul Scherrer demonstrated in this report, we have discovered many properties of crystals like salts, minerals, semiconductors and several organic molecules that wouldn't have been found otherwise.

XRC has been used to investigate the structure and purpose of various drugs, minerals and arguably most importantly DNA. By obtaining an X-ray crystallograph pattern of DNA (famously known as the B-form) Rosalind Franklin was able to prove the double helix structure commonly known today [2] giving rise to enormous progress in the field of genetics.

XRC is a very wide field of study however in the following set of experiments we will solely focus on three main methods and apply them to study common crystalline structures namely Sodium Chloride (NaCl), Lithium Fluoride (LiF), Potassium Bromide (KBr) and Silicon (Si). Due to the relatively primitive experimental setup of the original experiments we will conduct our experiments using a PHYWE X-Ray Unit to automise the data collection process letting us focus on the significant physical principles at hand.

Using Bragg's method, we will measure the dimensions of the unit cell (smallest volume of crystal that contains the symmetry of the structure) of a solid crystal allowing us to accurately calculate the density of the substance. Using Laue imaging of the same crystals, we will determine the symmetry of the unit cell. Additionally we will analyse the diffraction pattern to investigate how it was formed. Lastly, we will attempt to use the powder equivalents of the crystals to find the substance "fingerprint" to correctly identify the substances used.

2 Theory

A crystal structure consists of a three dimensional array of atoms composed of a basis repeated along a lattice. Due to the periodicity of the structure, there exist repeated planes of atoms within. As the spacing between these planes is typically in the order of magnitude of 1Å, X-rays have the ideal wavelength (10^{-10}m) for analysis of these structures via diffraction. X-rays scatter from the atoms in a crystal in a manner similar to that in which light waves are scattered from the ruled lines of a diffraction grating[3]. To achieve strong diffraction, the angle of incidence of x-rays must be equal to the angle of reflected x-rays for a set of planes.

$$\theta_i = \theta_r \tag{1}$$

The Bragg condition

$$n\lambda = 2dsin\theta \tag{2}$$

(where d is the spacing between planes, θ is the angle between the incident ray and the plane and λ is the wavelength of x-rays being shone on the crystal) must also be satisfied.

Crystal structures can be arranged in one of fourteen different possible Bravais lattices one of which the Face Centered Cubic (FCC) is shown in 1. These

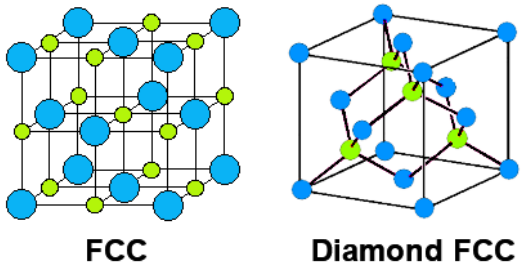

Figure 1: Diagram of a FCC (NaCl) and Diamond FCC (Si) crystal structures [5]

lattices have different sets of parallel planes indicated by miller indices which are simply planes created by the atoms inside. For a cubic lattice, such as the one shown in 1, these miller indices (hkl) can help determine the relationship between the spacings between subsequent planes and the length of a side of a unit cell (smallest group of atoms that has the symmetry of the crystal) a. For the purpose of this discussion we will focus only on the FCC and Diamond FCC structures.

$$d = \frac{a}{\sqrt{h^2 + k^2 + l^2}} \tag{3}$$

Miller indices are given as the vector (hkl) of a plane in the unit cell of the structure. Compared to a simple cubic structure with 8 lattice points, an FCC structure will have extra atoms in between. This means that it not only can have (100) indices but also (200) where the space in between the planes is a half.

We can obtain Bragg's law via the geometry of the path difference of the X-rays passing through the crystal. 2. For constructive interference, the extra distance (path difference) travelled by the X-ray being reflected by the second plane must be equal to $n\lambda$ where n is an integer.

$$n\lambda = AB + BC \tag{4}$$

Seeing as AZB is a right angled triangle with d as the hypotenuse we can deduce that:

$$AB = dsin\theta \tag{5}$$

Because AB is equal to BC, Equation 4 becomes $n\lambda = 2AB$ which when combined with Equation 5 gives Equation 2.

Following this relation we see that both the distance between planes and the wavelength of the X-ray depend on the angle of reflection. Consequently if both λ and the angle θ are known it is possible to measure the space between between planes d. Furthermore, we can then extract the lattice constant a which leads to the dimensions of the cubic unit cell and therefore density of the crystal.

Laue Imaging works on the same principle with a bit more involved analysis. When passing X-rays directly through a crystal orientated in a known direction, the X-rays will diffract through the crystal at

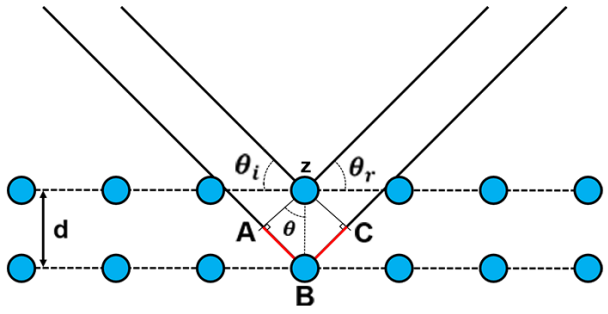

Figure 2: Geometrical description of X-rays being diffracted from two planes inside a crystal. ABC shows the path difference (in red) travelled by the x-rays being reflected from the second plane which then interfere with the first ray. (Created Using ImageJ & Photoshop)

different angles due to reflection from different principle axes (planes of high atom density).

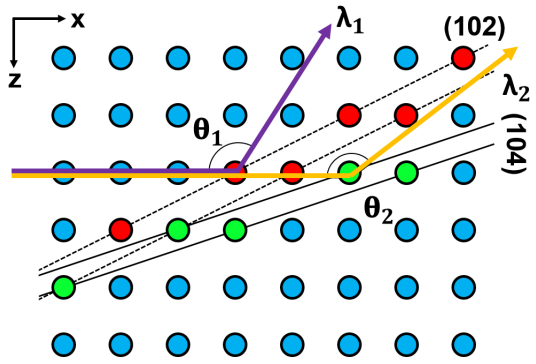

Figure 3: Diagram illustrating how Laue Spots are generated when shining a collimated X-ray beam at a crystal of a known orientation. Dotted line (red atoms) corresponds to the (102) plane and the solid (green atoms) to the (104) plane. As seen, the plane spacing between d is smaller for the (104) plane (See Equation 3). Created Using ImageJ & Photoshop

Figure 3 demonstrates a beam of X-rays passing through a crystal directly and diffracting at different angles. In a real case scenario this would be a 3D crystal (including the y axis) meaning the pattern created would be visible through 360° and would be visible on a flat projection screen (obtained using the Laue Method). Each principle plane in the crystal would be visible as a spot on the screen where the intensity of the spot is directly proportional to the atom density of the plane as the diffraction is stronger. The diffraction pattern obtained from such a setup gives us insight into the symmetry of the unit cell of the crystal as well as the type of lattice structure. For an FCC structure the identified planes should have miller indices (hkl) either all even (220) or all odd (110), whereas for a Body Centered Cubic BCC they could be any combination [6]. By applying the theory of multiple slit diffraction [7] to a 1 atom thick 2D crystal structure we would expect that the pattern created is simply the reciprocal lattice (or Fourier transform) of the crystal structure itself. This means that in theory we could apply an Inverse Fourier Transform to the diffraction pattern and obtain an image of the crystal structure itself. Although theoretically this should work in practice with materials such as graphene, if the crystal is not exactly 1 atom thick, the phase information of the lattice structure is lost. This means the projection is no longer an accurate representation of the reciprocal lattice meaning we cannot retrieve this information using an Inverse Fourier transform.

For a sample of a crystal in a powdered form, when an X-ray beam is passed through, the diffraction pattern is no longer restricted to one orientation of the crystal or to put it simply it all orientations of the crystals are present. In this case the diffraction pattern should become "smudged" Debye-Scherrer rings [8]. Because all of the possible orientations of the crystal are present in the powder, all of the possible planes for the crystal structure should theoretically be present in the form of rings where each ring corresponds to a plane. Once again, this image contains information which is used to characterise the structure of the crystal.

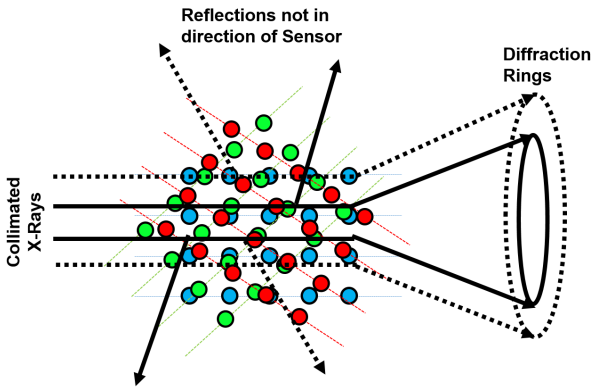

Figure 4: Diagram illustrating the geometry of X-Rays passing through a powdered crystal. Different coloured atoms correspond to planes orientated. Smaller angles of diffraction lead to rings of smaller radius. Created Using ImageJ & Photoshop

3 Method

3.1 Bragg's Method

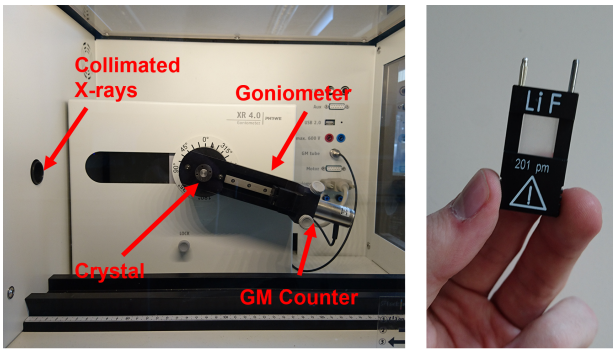

Goniometer/ Geiger Muller Tube Setup LiF Crystal Sample

Figure 5: Experimental Setup of Bragg's Method consisting of a Molybdenum X-Ray source, Rotating Goniometer at a 1:2 angle ratio with a Geiger-Muller tube as illustrated.

Before beginning the experiment we obtained a set of samples of common salts of known orientations (cleaved along known miller planes) that had a casing compatible with the X-Ray Unit (As shown on the right in Figure 5). We turned the unit on, plugged it into the computer using a Type A to Type B USB cable and started the PHYWE Measure software. Next, we placed the crystal sample in the placeholder and closed the transparent door of the X-ray unit to prevent exposure to radiation. Next, in the software we adjusted the goniometer to a 1:2 Coupling mode which locked the ratio of the angle of the crystal and the angle of the GM Tube to 1:2 so that the first condition of strong diffraction Equation 1 was satisfied at all times.

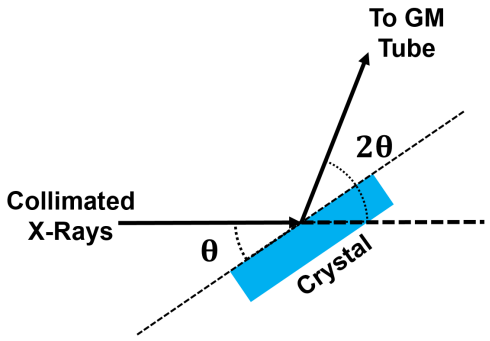

Figure 6: Illustration of how the goniometer was setup to satisfy the condition that incident angle must be equal to the reflection angle. Created Using ImageJ & Photoshop

Holding all of the other variables of Equation 2 constant, the goniometer slowly rotated the crystal (increased θ) in even intervals for a range of angles stopping at each angle to count the radiation intensity for an integration time t which was then recorded by the software. As these parameters depend on the samples being measured we decided to change them to suit our purpose. The parameters we used for all of the samples are as follows: Angle interval = 0.1°; Angle range = 3-30°; integration time = 4s (18min for whole range). The X-Ray tube anode voltage and current were set to 35kV and 1mA respectively as suggested by the PHYWE manual [9]. We then used the inbuilt automated calibration of the software by choosing the crystal being measured and simply pressing "Calibrate" to locate the correct start and end positions

of the scan range. In the program we then plotted the count against angle to produce a spectrogram. We then repeated this for crystals: NaCl (100), NaCl (110), NaCl (111), LiF (100), KBr (100) & Si (100) calibrating the apparatus to the appropriate crystal each time.

In addition to changing the parameters of the goniometer to get a high quality spectrogram, we experimented with changing the voltage of the anode of the X-ray tube and adding filters to the collimator to see if we could improve our results. For this we decided to only use the LiF (100) sample to keep our investigation consistent and cut down on time.

3.2 Laue Method

Figure 7: Experimental setup inside the X-Ray Unit for the Laue method experiment.

Using a different PHYWE X-Ray unit equipped with an XRIS Sensor and connected to a computer running PHYWE Measure CT software, we fitted one of the crystal samples at the collimator as seen in Figure 7 and adjusted the distance between the crystal and the XRIS sensor to 9 cm as recommended by the PHYWE manual [9] using the sliding rail with a scale. Next, after closing the door and locking it, we used the Measure CT software to take multiple exposures using the sensor with the X-Rays turned off to create an offset image allowing us to account for background radiation it may be picking up. We then saved this file as a .tiff image which is a raw image format allowing us to change the exposure after the picture has been taken. Next, we turned the Tungsten X-Ray source on and proceeded to take the exact same number of exposures at the same exposure time and saved the file in the same format. We then used the inbuilt feature of the software to use the offset (Image with X-rays turned off) to account for background radiation in the actual image, adjusted the exposure of the final image until all spots were visible with minimal noise and saved it as a .png image for further analysis.

Due to the nature of the program (which was not created with this experiment in mind), we had to set an exposure time for which the sensor would be collecting light for for each exposure and use a stopwatch to measure how long the entire measuring process took place to work out the number of exposures taken. For example, with an exposure time of 10 seconds we would collect data for 60 seconds giving us a total of 6 exposures. The only indicator of an exposure being complete is a blink on the software which would frequently glitch making it an unreliable method of collecting data.

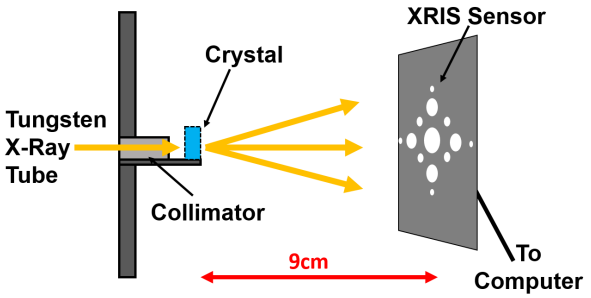

Figure 8: Illustration of experimental setup of Laue Method experiment where x-rays are diffracted through a crystal and captured by an PHYWE XRIS sensor 9 cm away connected to a computer running Measure CT software. Created Using ImageJ & Photoshop

After some experimentation with the variables of the sensor we decided to use the following parameters of the sensor: Exposure time = 10 s; Measure time = 3

min; Resolution = 500×500px. When the exposure time was too low, the spots were dim and if it was too high there was a lot of noise. Measure time did not have a significant enough effect on the final image to increase it further. Higher resolutions made the entire image dimmer as due to an increased number of pixels, each point on the sensor collected less photons over the same amount of time.

To further improve the quality of our images we decided to use a lead shield in place of the middle spot to prevent overexposure of the sensor allowing it to pick up dimmer spots.

3.3 Debye-Scherrer Powder Method

This experiment was carried out using the exact same experimental setup as demonstrated by Figure 8 but instead of a crystal, the X-rays were passed through a powdered crystal. To powder the crystal we used a mortar and pestle to crush up a solid crystal into fine dust. In our preliminary research of the method [10], we found that it is best to crush up the powder for at least an hour to obtain better results so we decided to crush it for 2 hours.

Figure 9: Image of powder sample attached to the collimator using blu-tack inside the X-Ray unit for the powder diffraction experiment. Collimator was taken out entirely to ensure the powder lined up with the incident x-rays.

To contain the powder we put it inside a piece of cardboard with a hole, hole punched through it and secured the powder inside with sellotape Figure 9. We chose sellotape as it would not interfere with the diffraction pattern of the crystalline structure as it is an amorphous material through which X-Rays can pass freely. We made sure to label the piece of cardboard with the correct substance that was inside for future reference. We then attached the sample to the collimator using blu-tack. After adjusting the distance between the sample and the sensor to the correct position we proceeded to take images in the same way as in Section 3.2 with the same sensor parameters. We repeated this process for: Lithium Fluoride (LiF), Potassium Bromide (KBr), Quartz, Sodium Chloride (NaCl) and regular off the shelf sea-salt.

To take this experiment even further and to see whether a really thin crystalline structure would produce a pattern that resembles the reciprocal lattice we used the rather primitive "scotch-tape method" [11] of producing "graphene" using graphite from a pencil and the sellotape from before.

4 Results & Analysis

4.1 Bragg Analysis

Upon first inspection of a spectrogram obtained using the Bragg method (As illustrated by Figure 10) with a molybdenum X-ray source we see the characteristic repeating double peaks (especially in the 6-9° range). This is due to the source having two distinct electron transitions resulting in X-Rays of two wavelengths λ_1=71.08 pm & λ_2=63.09 pm labelled on the diagram. In order to determine the lattice constant of the crystal we substitute Equation 3 into Equation 2 and rearrange to get

$$a = \frac{n\lambda \cdot \sqrt{h^2 + k^2 + l^2}}{2\sin\theta} \tag{6}$$

which makes the analysis easier. Now by simply identifying the peaks and their corresponding values of (hkl), n, λ and θ for each one of the crystals we are able to calculate the lattice constant. Furthermore, we can calculate the density of the substance by calculating the volume of unit cell ($V_o = a^3$ For cubic

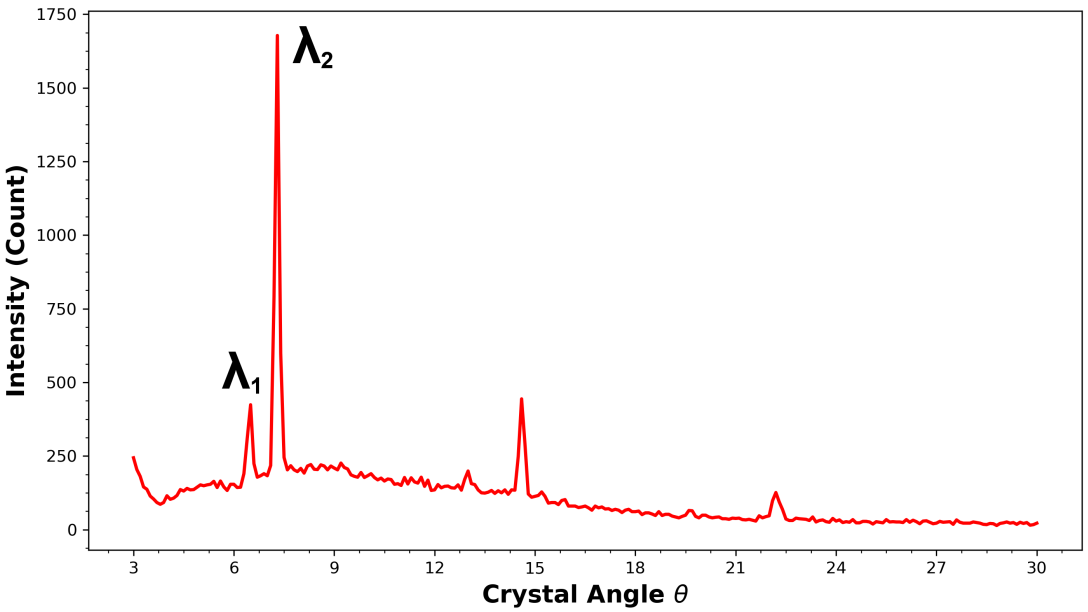

Figure 10: Spectrogram of NaCl (100), Gate Time = 4 s. λ_1 and λ_2 correspond to the two different wavelengths created by electron transitions in the the molybdenum X-ray source. Plotted using Python 3.6.

structures) and dividing the sum of the mass of all atoms (found in periodic table) inside the unit cell by V_o.

$$\rho = \frac{\sum_i^N m_i}{V_o} \tag{7}$$

Where N is the number of atoms and m is their atomic mass in kg. For each peak on the spectrogram we worked out the lattice constant and the corresponding density to go along with it then averaged them giving us a value of ρ and a for each crystal measured.

The experimental values obtained using this method were not far from the actual values with an average error of 11%. The experimental values of the NaCl (111) sample seem to be outliers as in comparison to the other values it has an error of 21.1%. This can be caused because of two reasons. Firstly, when we obtained the spectrogram for this sample, there was an additional double peak beginning at 3° which is the first angle we measured. The intensity of this peak was low enough that we decided to ignore it and use the next double peak for the first order of diffraction. Despite re-calibrating the X-Ray Unit and doing the experiment again, we were still getting this result and concluded that this must be due to an imperfection in the crystal as upon further inspection we did see that the crystal had quite a few smudges. Another possible reason for this would be variation between samples, although this is unlikely as the crystals came from the same source, random wear and tear may have some crystals more than others. The crystals in the table are sorted by the order of the mass of atoms inside the unit cell with M_{NaCl}=9.70×10^{-26} kg, M_{LiF}=1.72×10^{-25} kg & M_{KBr}=7.87×10^{-25} kg [12]. Although the density seems to be increasing proportionally with the increase in unit cell mass however the lattice constant

Crystal	a_{ex} ($\mathring{A}$)	ρ_{ex} ($\mathbf{gm^{-3}}$)	a_{ac} ($\mathring{A}$)	ρ_{ac} ($\mathbf{gm^{-3}}$)
NaCl (100)	3.4275±0.0117	2.4101±0.0001	5.64	2.16
NaCl (110)	3.4982±0.0128	2.2669±0.0001	-	-
NaCl (111)	3.8473±0.0201	1.7041±0.0001	-	-
NaCl (avg)	3.5910±0.0149	2.0957±0.0001	-	-
LiF (100)	3.8671±0.0248	2.9656±0.0002	4.02	2.64
KBr (100)	7.0182±0.0498	2.2767±0.0006	6.59	2.75

Table 1: Table showing experimental value of the lattice constant a_{ex} and density ρ_{ex} as well as the actual values a_{ac} and ρ_{ac} obtained from the Crystallography Open Database [12]. Actual value columns for Sodium Chloride are blanked out as they are independent of the orientation of the principle plane measured meaning they're all the same as NaCl (100).

of Lithium Fluoride LiF seems to break the trend with the increase in lattice constant. This is most likely due to the fact that Lithium Fluoride has the least massive atoms in its unit cell. The atomic numbers of Lithium and Fluorine are 3 and 9 respectively compared to Sodium and Chloride which have atomic numbers 11 and 17 or even Potassium and Bromine, 19 and 35.

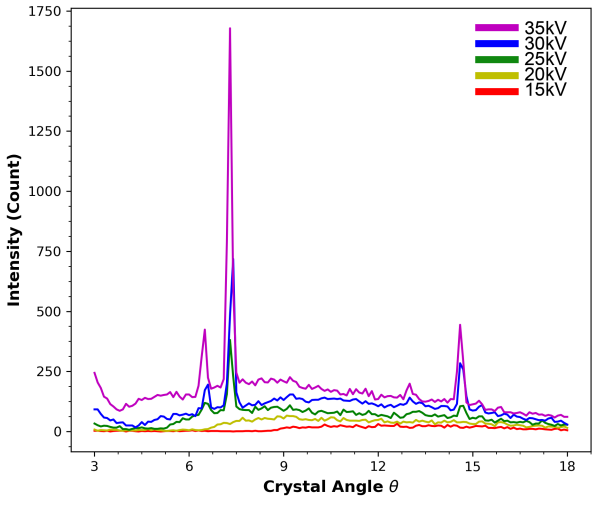

Figure 11: Plot of NaCl (100) with Gate time of 2 sec for various X-ray anode voltages. (Gate time decreased due to wide range) Plotted using Python 3.6

By varying the voltage in the range from 15kV to 35kV we attempted to find the ideal anode voltage for this experiment. What we found is that decreasing the voltage decreases the intensity of the Bremsstrahlung radiation and the K-lines proportionally. The K-lines seemed to decrease faster than the breaking radiation until they were not visible anymore at even 20kV (5kV change caused the count rate to half). Decreasing the voltage like this helps us see the trend in increasing the Voltage and if we mentally extrapolate this trend to higher voltages it is clear that increasing the voltage past 35kV would be beneficial in distinguishing peaks of higher order such as the one located at 12.6°. Unfortunately we were instructed not to increase the voltage of the equipment given as it may cause damage to the GM tube. In a similar experimental setup with more durable equipment this would definitely be a good parameter to look optimise for better results.

Adding filters to the collimator had a significant effect on the clarity of the K-lines. As demonstrated by Figure 12. Applying a Nickel filter had a dramatic effect on the breaking radiation for higher crystal angles with not much effect on the peak itself. The most intense peak demonstrates how much radiation is prevented from reaching the GM Tube. The Zirconium Filter was too intense for the molybdenum X-Ray tube and voltage, and we believe is more designed for the Tungsten anode however we were not allowed to switch out the X-ray tube in the unit. If we were to repeat this experiment, the ideal setup for analysis would be a higher anode voltage combined with

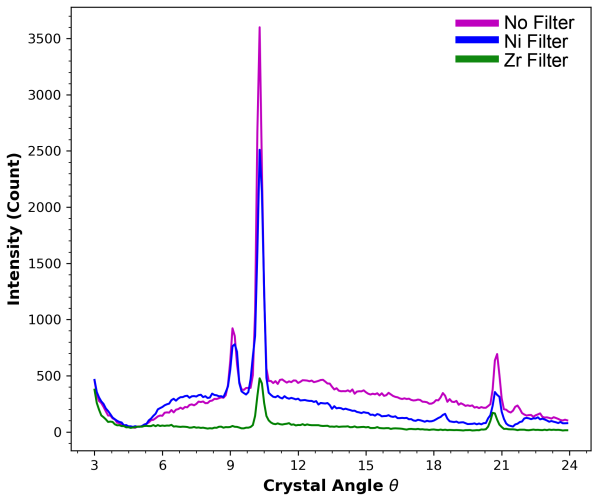

Figure 12: Plot of LiF (100) using a collimator with no filter, a Nickel (Ni) filter and a Zirconium (Zr) filter. Plotted using Python 3.6

the Nickel filter which would reduce the background radiation more whilst maintaining intense peaks allowing us to study even higher orders of diffraction. A higher integration time would also be beneficial if time permits.

4.2 Laue Analysis

After obtaining the diffraction pattern images we decided that it was helpful to invert the colour of the images to make the Laue spots easier to see. The symmetry of the patterns is immediately distinguishable at first sight which was a great indicator of the orientation of the crystal [eg. all (100) orientated crystals have a 4-fold symmetry].

To determine the miller indices of the planes responsible for the Laue spots present we generated a list of all possible values of (hkl) for an FCC structure (where they are either all even or all odd) using a simple Python script and cut off the list for values of $h^2+k^2+l^2$ higher than 44 (equivalent to the (622) plane). Next using Excel we calculated the: Bragg angle θ, corresponding wavelength λ and the ratio of k/l for each one of the (hkl) combinations. Next we used the relation

$$\lambda_{min} = \frac{hc}{eV} \tag{8}$$

to eliminate wavelengths that could not physically be created with an anode voltage of 35kV. We also eliminated the values of (hkl) that gave a Bragg angle higher than the 36.87° allowed by the geometry of the experiment with a 6 cm wide sensor 9 cm away from the crystal. Furthermore, we used ImageJ to measure the number of pixels the spots are away from the center allowing us to find the physical distance by multiplying this number by the corresponding physical distance 96μm/px which gave us the Bragg angle of the spot. These variables along with the relation

$$\frac{k}{l} = \frac{y}{z} \tag{9}$$

helped us narrow down and identify several spots on the NaCl (100) and LiF (100) images. After the analysis of the data we found that the sensor was too close in the LiF (100) example meaning we missed out some spots which could have been identified (this was the second time we took measurements as we redid the entire experiment using a lead shield meaning we couldn't repeat). In this experiment we did not get any diffraction pattern for the KBr Sample which is why it is missing. The diffraction image for silicon has visible horizontal lines due to overdoing the offset on the image however it demonstrates nicely how the offset method works.

4.3 Debye-Scherrer Analysis

Due to the primitive nature of obtaining a good sample we were not able to achieve the Debye rings predicted by theory. We did however find out about the effect of how fine the powder is on the pattern visible. Additionally, we decided to compare the Sodium Chloride sample available in the lab to ordinary kitchen salt from home to find similarities and differences between the two.

In Figure 14 the Sodium Chloride diffraction pattern features a faint blurry ring around the center

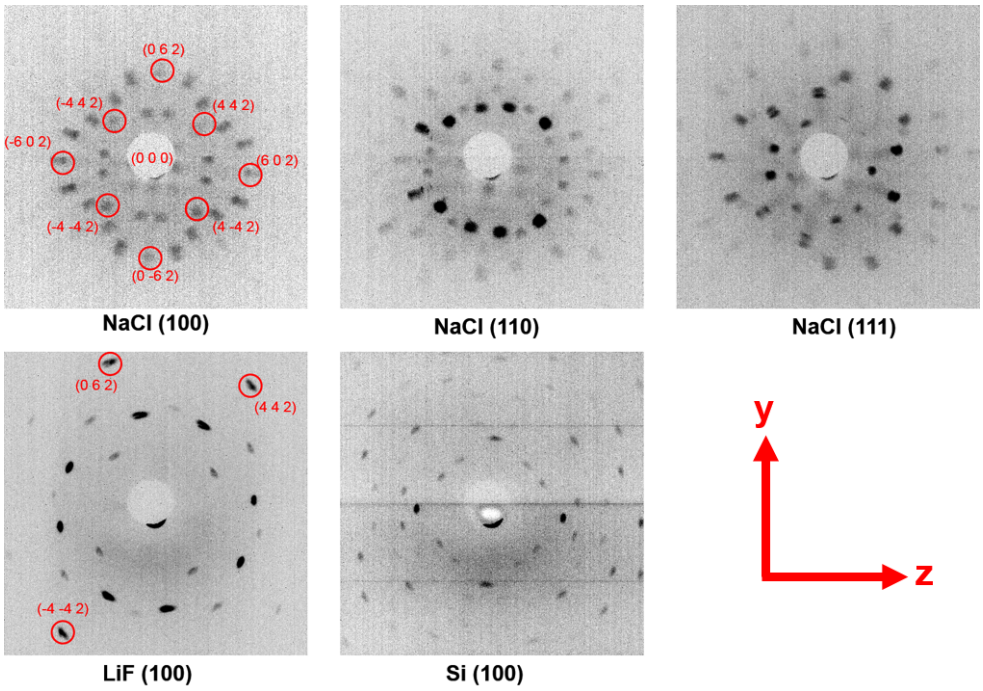

Figure 13: Resulting Diffraction patterns of the Laue Imaging method and the spots identified using the method of elimination based on diffraction conditions circled in red. Exposure time = 10 sec; Measure time = 3 min; Resolution = 500×500px

with some seemingly random spots on top of it. As this is the most finely ground up crystal we used, we theorise that this might be some of the Debye rings smudged together. Comparing this to the kitchen salt (which wasn't as well ground up) diffraction pattern which even seems to exhibit symmetry suggest that some planes still have higher atom densities than others meaning the sample was not ground up enough however this is strictly speculative as this data does not contain enough information to provide solid conclusions. For the Quartz powder we used a sample ground up by another group some time before carrying out this experiment as a preliminary test to see what we would see. What we found was quite a periodic and structured pattern leading us to believe that over time, the powder experienced compression from being stored which caused it to retain some of its original structure. At first the Lithium Fluoride sample gave no diffraction pattern at all so we decided to retake the image without a lead shield to see the fainter details however we still could not observe any rings.

The "scotch-tape graphene" method was unsuccessful as shining X-Rays at it even without a lead shield did not produce a pattern on the sensor. Additionally, the KBr sample provided no visible diffraction pattern leading us to believe a higher exposure time was needed.

5 Conclusion

In Summary, we determined the lattice constants and densities of common crystals to a satisfactory level using the Bragg method. We attempted to find the ideal parameters to help distinguish the peaks of the spectrograms more by varying the voltage of the X-

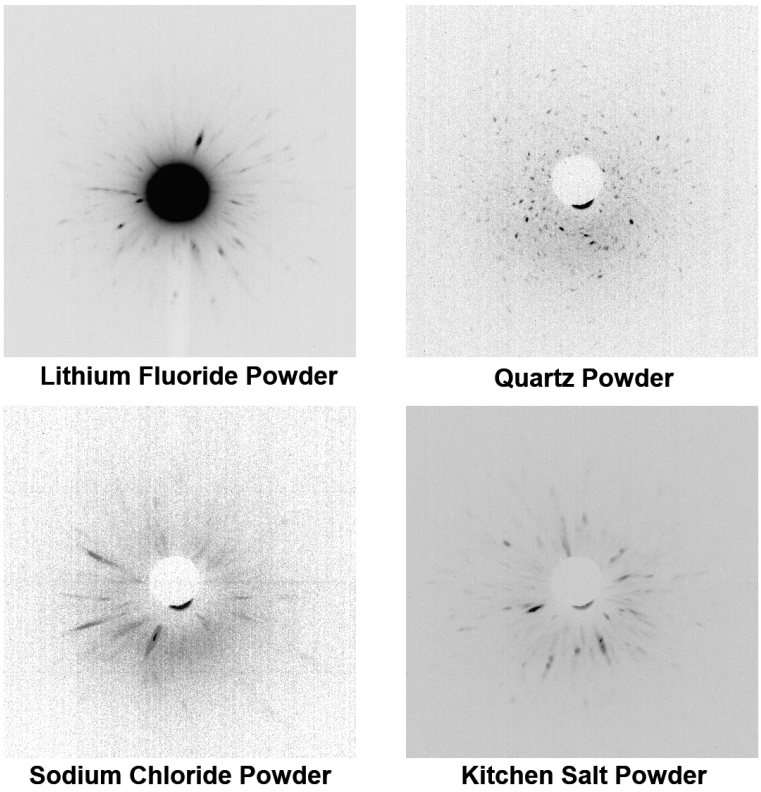

Figure 14: Resulting diffraction patterns using the Debye-Scherrer method. Exposure time = 10 sec; Measure time = 3 min; Resolution = 500×500px

ray anode as well as testing out collimator filters which we found to be somewhat helpful. We did run into a few limitation with the experiment though. Firstly, the smallest angle increment the goniometer allowed for was 0.1° limiting the resolution of our plot making uncertainties very inaccurate. Additionally, we were limited to the crystals given to us that have also been handled by others in the lab making them not an accurate representation of pure crystals. Also due to this we were not able to study solid crystals from outside the lab without damaging the sample casing. The software also did not have a setting to measure the spectrogram of Silicon and didn't have an option to manually enter the parameters limiting us with what we could do with the experiment.

We were able to successfully obtain the Laue images of Sodium Chloride, Lithium Fluoride and Silicon and analyse these to confirm that they are in fact of the FCC structure judging by the symmetry and the Laue spots identified. The method of finding spots was quite limiting as even with all of the conditions satisfied we were unable to identify some spots. The KBr (100) Crystal also showed no diffraction pattern at all which was either due to the principle axes being oriented in such a way that constructive interference was impossible or the massive atoms in the structure simply required the exposure time to be increased. The software used was extremely clunky and tedious to use with several features not implemented correctly such as the lack of a count of how many exposures have been taken which would prevent poor offsets such as the one seen in the Silicon image found

in Figure 13.

Although the results of the Debye-Scherrer powder experiment were underwhelming and was very difficult to achieve meaningful data, the technique of preparing a sample was carried out correctly and given enough time the equipment used in this experiment can be used to attempt it again using a higher exposure time and no lead shielding. The idea of creating a 1 atom thick crystal structure to later analyse using a reverse Fourier transform is certainly possible however would require a much more precise sensor and a really high exposure time.

References

[1] Bragg WL, *The Structure of Some Crystals as Indicated by their Diffraction of X-rays*, Proc. R. Soc. Lond 1913,248–275

[2] Klug, A, *Rosalind Franklin and the Double Helix*, 1974 Nature, pg. 787–788

[3] N.F.M Henry, H. Lipson W.A. Wooster, *The Inerpretation of X-ray Diffraction Photographs*, Macmillan & CO LTD, 1960. pg. 71-73

[4] Charles Kittel *Introduction to Solid State Physics* John Wiley & sons Inc. Fourth Edition 1971. pg.19-56

[5] `https://www.tf.uni-kiel.de/matwis/amat/iss/kap_4/illustr/i4_2_1.html` Accessed 10/02/19

[6] M.M. Woolfson *X-Ray Crystallography* Cambridge University Press, 1970. pg. 57

[7] Thomas Young, *The Bakerian Lecture: Experiments and calculations relative to physical optics*, Philosophical Transactions of the Royal Society of London, pg. 1–16

[8] `http://pd.chem.ucl.ac.uk/pdnn/diff2/kinemat2.htm`,Accessed 10/02/19

[9] `http://www.phywe.net/wp-content/uploads/00298-02_Phywe_XRay_englisch.pdf` Accessed 12/02/19

[10] L.J. Poppe, V.F. Paskevich, J.C. Hathaway, *A Laboratory Manual for X-Ray Powder Diffraction*, U. S. Geological Survey Report 1-41

[11] Jun Zhu, *Graphene Production: New solutions to a new problem*, Nature Nanotechnology volume 3, pages 528–529 (2008)

[12] `http://www.crystallography.net/cod/browse.html` Accessed 14/03/19

[13] https://www.phywe.com/en/compton-scattering-of-x-rays.html (Accessed 14/02/19)

[14] H.S. Lipson, *Crystals and X-rays*, Wykeham Publications LTD, 1970. 13-53

[15] J.R. Hook, H.E. Hall *Solid State Physics*, John Wiley & Sons 1991. pg 1-22